Latest DVCS Results from HERMES

Sergey Yaschenko for the HERMES collaboration

DESY, Platanenallee 6, D-15738 Zeuthen, Germany

Hard exclusive leptoproduction of real photons on nucleons and nuclei, Deeply Virtual Compton Scattering (DVCS), is one of the theoretically cleanest ways to access Generalized Parton Distributions (GPDs). During 1996–2006 the HERMES experiment at DESY, Hamburg, collected data on DVCS utilizing the HERA polarized electron or positron beams with energies of 27.6 GeV, and longitudinally and transversely polarized or unpolarized gas targets (H, D or heavier nuclei). The azimuthal asymmetries measured in the DVCS process allow access to the imaginary and/or real part of certain combinations of GPDs. An overview of the latest HERMES results on DVCS is presented.

1 Introduction

The theoretical framework of Generalized Parton Distributions (GPDs) includes Parton Distribution Functions and Form-Factors as limiting cases and moments of GPDs, respectively, and can provide a three-dimensional representation of the structure of hadrons at the partonic level. GPDs depend on three kinematic variables: the squared four-momentum transfer t to the nucleon and x and ξ, which represent respectively the average and half the difference of the longitudinal momentum fractions carried by the probed parton in initial and final states. For the proton, there are four twist-2 GPDs per quark flavor: H_q, E_q, $\widetilde{H}_q$ and $\widetilde{E}_q$. Among other hard exclusive processes, Deeply Virtual Compton Scattering is one of the theoretically cleanest ways to access GPDs. DVCS is experimentally indistinguishable from the electromagnetic Bethe-Heitler (BH) process because they share the same final state. The real photon is radiated (Fig. 1) from the struck quark in DVCS, or from the initial or scattered lepton in BH.
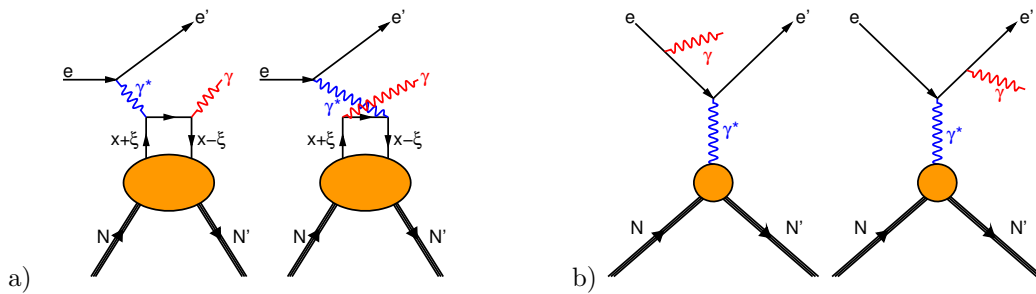

Figure 1: Leading order diagrams for the deeply virtual Compton scattering (a) and the Bethe–Heitler (b) processes.

The cross section of the exclusive photoproduction process can be written as [1]

$$\frac{d\sigma}{dx_B dQ^2 dt d\phi} = \frac{\alpha^3 x_B y}{16\pi^2 Q^2 e^3} \frac{2\pi y}{Q^2} \frac{|T_{DVCS}|^2 + |T_{BH}|^2 + I}{\sqrt{1 + 4x_B^2 M_N^2/Q^2}},$$ (1)

where T_{DVCS} (T_{BH}) is the DVCS (BH) amplitude, I is the interference term, x_B is the Bjorken scaling variable and $-Q^2$ is the squared four-momentum transferred by the virtual photon. The amplitude of the BH process can be precisely calculated from measured elastic form factors of the nucleon. The BH process dominates at HERMES kinematics. However, the kinematic dependences of the cross section terms generate a set of azimuthal asymmetries which depend on the azimuthal angle ϕ between the real-photon production plane and the lepton scattering plane.

2   Azimuthal Asymmetries in DVCS

The cross section for a longitudinally polarized lepton beam scattered off an unpolarized proton target σ_{LU} can be related to the unpolarized cross section σ_{UU} by

$$\sigma_{LU}(\phi; P_B, C_B) = \sigma_{UU}(\phi) \cdot \left[1 + P_B A_{LU}^{DVCS}(\phi) + C_B P_B A_{LU}^I(\phi) + C_B A_C(\phi) \right],$$ (2)

where A_{LU}^I (A_{LU}^{DVCS}) is the charge (in)dependent beam-helicity asymmetry (BSA) and A_C is the beam charge asymmetry (BCA), $C_B(P_B)$ denotes the beam charge (polarization). In the analysis effective asymmetry amplitudes are extracted, which include ϕ dependencies from the BH propagators and the unpolarized cross section. Each asymmetry can be expanded in a Fourier series in ϕ as

$$A_{LU}^I(\phi) = \sum_{n=1}^{2} A_{\text{LU,I}}^{\sin(n\phi)} \sin(n\phi) + \sum_{n=0}^{1} A_{\text{LU,I}}^{\cos(n\phi)} \cos(n\phi),$$ (3)

$$A_{LU}^{DVCS}(\phi) = \sum_{n=1}^{2} A_{\text{LU,DVCS}}^{\sin(n\phi)} \sin(n\phi) + \sum_{n=0}^{1} A_{\text{LU,DVCS}}^{\cos(n\phi)} \cos(n\phi),$$ (4)

$$A_C(\phi) = \sum_{n=0}^{3} A_{\text{C}}^{\cos(n\phi)} \cos(n\phi) + A_{\text{C}}^{\sin\phi} \sin\phi.$$ (5)

By combining the data taken with different beam charges and helicities, the amplitudes were fitted simultaneously using a Maximum Likelihood method described in detail in Ref. [2]. In the case of unpolarized beam and transversely polarized target, the transverse target-spin azimuthal asymmetry (TTSA) can be measured, which in addition to ϕ also depends on the angle ϕ_S between the lepton scattering plane and the direction of the target polarization vector.

3   Experiment and Data Analysis

The HERMES experiment [3] utilized longitudinally polarized 27.6 GeV electron/positron beams of the HERA storage ring at DESY together with longitudinally and transversely polarized or unpolarized gas targets (H, D or heavier nuclei). Exclusive events were selected requiring the detection of exactly one scattered lepton and of exactly one photon. In addition, as the recoiling

proton has not been detected, the missing mass was required to match the proton mass within the resolution of the spectrometer, which defines the "exclusive region". Without recoil proton detection it is not possible to separate the elastic DVCS/BH events from the "associated" process, where the nucleon in the final state is excited to a resonant state. Within the exclusive region, its contribution is estimated from a Monte Carlo simulation to be about 12%, which is taken as part of the signal. The main background contribution of about 3% is originating from semi-inclusive π^0 production and is corrected for. The contribution from exclusive π^0 production is estimated to be less than 0.5%. The systematic uncertainties are obtained from a Monte Carlo simulation estimating the effects of limited acceptance, smearing, finite bin width and alignment of the detectors with respect to the beam. Other sources are background contributions and a shift of the position of the exclusive missing mass peak between the data taken with different beam charges.

4 Results

In Figures 2 and 3 results obtained with the hydrogen target are shown [4]. The first four rows of Fig. 2 represent different cosine amplitudes of the BCA, whereas the last row displays the fractional contributions of the associated BH process. In the first column the integrated result is shown, in the other columns the amplitudes are binned in $-t$, x_B or Q^2. The error bars show the statistical uncertainties and the bands the systematic uncertainties. The magnitudes
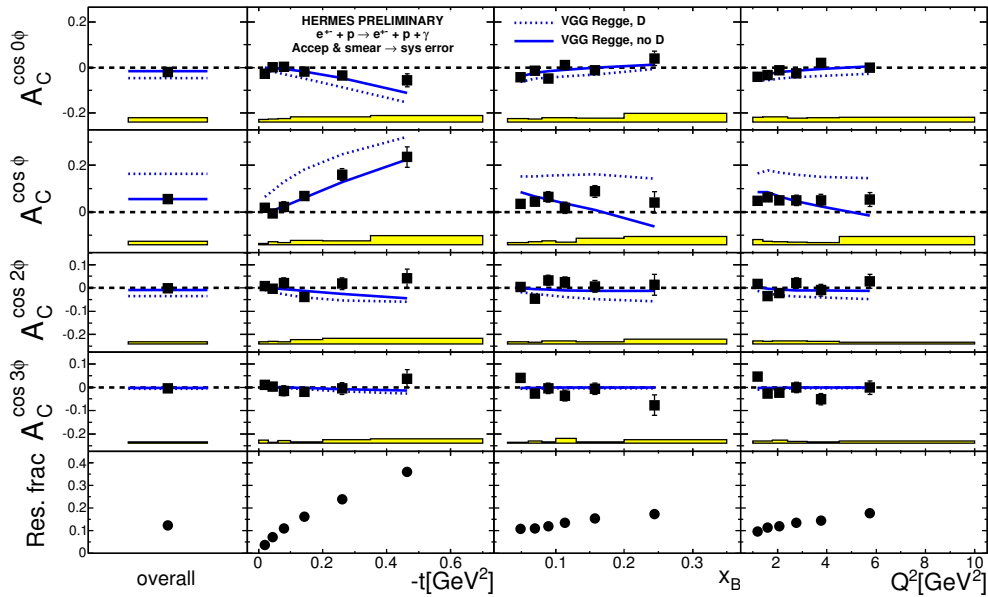

Figure 2: The amplitudes of the beam charge asymmetry extracted from hydrogen data (black bullets) [4]. The error bars (bands) represent the statistical (systematic) uncertainties. The curves are predictions of a double-distribution GPD model [6].

of the first two cosine moments $A_C^{\cos 0\phi}$ and $A_C^{\cos\phi}$ increase with increasing $-t$, with opposite signs, in agreement with theoretical expectations. In HERMES kinematics, both relate to the real part of the GPD H, but the constant term is suppressed relative to the first moment. The second cosine moment appears in twist-3 approximation and is found to be compatible with zero like the third cosine moment, which is related to gluonic GPDs. The first sine moment $A_{LU,I}^{\sin\phi}$ is large and negative in the covered kinematics (see Fig. 3). This amplitude relates to the imaginary part of the GPD H. Also shown in the figures are GPD model calculations based on the framework of double distributions [6]. The model includes a Regge-inspired t-ansatz and a factorized t-ansatz. The BCA amplitudes favour the double-distribution model with a Regge-inspired t-dependence, if the D-term is neglected. Both model calculations fail to describe the data except for small $-t$. The charge-independent BSA moments are found to be compatible with zero. Results obtained with a deuterium target (see Fig. 4) are found to be consistent in most kinematic regions [5]. The proton and deuteron results for the amplitude $A_{LU,I}^{\sin(2\phi)}$ integrated over the acceptance differ by 2.5 sigma for the total experimental uncertainties. This possible discrepancy is most evident at large $-t$ or large x_B (or Q^2) and has no obvious explanation.
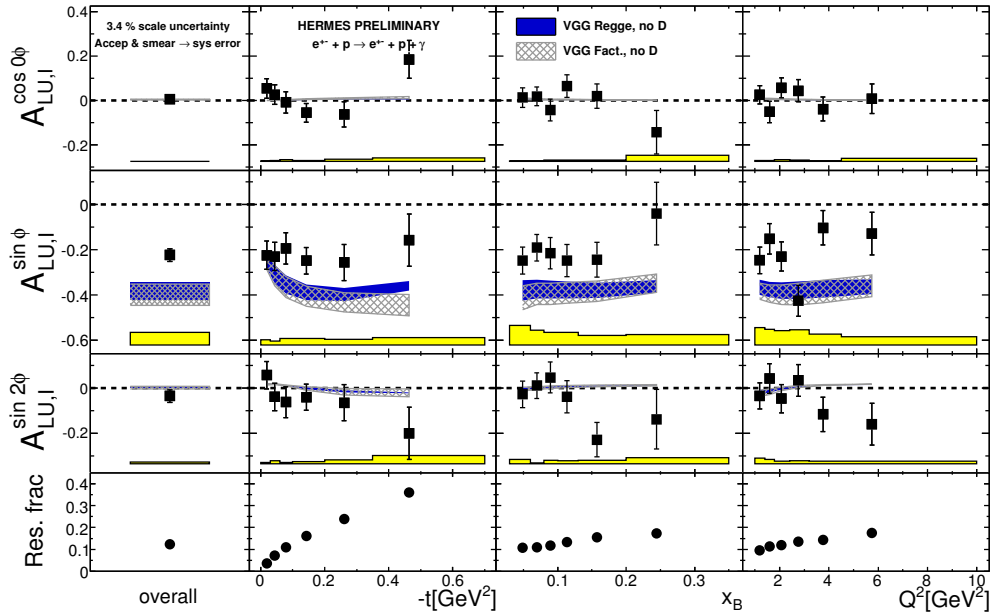

Figure 3: The amplitudes of the beam-helicity asymmetry from the interference term on the unpolarized hydrogen target [4]. The error bars (bands) represent the statistical (systematic) uncertainties. The curves are predictions of a double-distribution GPD model [6].

For data taken with the transversely polarized target, the beam charge asymmetry $A_C(\phi)$ and the TTSAs $A_{UT}^{DVCS}(\phi)$ and $A_{UT}^I(\phi)$ from DVCS and interference term, respectively, have been extracted simultaneously. By comparing GPD model calculations [6] with the measured BCA and TTSA, a model-dependent constraint on the total angular momenta carried by up- and down- quarks of the nucleon is obtained as $J_u + J_d/2.8 = 0.49 \pm 0.17\,(\exp_{tot})$ [2]. However, the double-distribution model of [6] cannot explain all existing DVCS data.
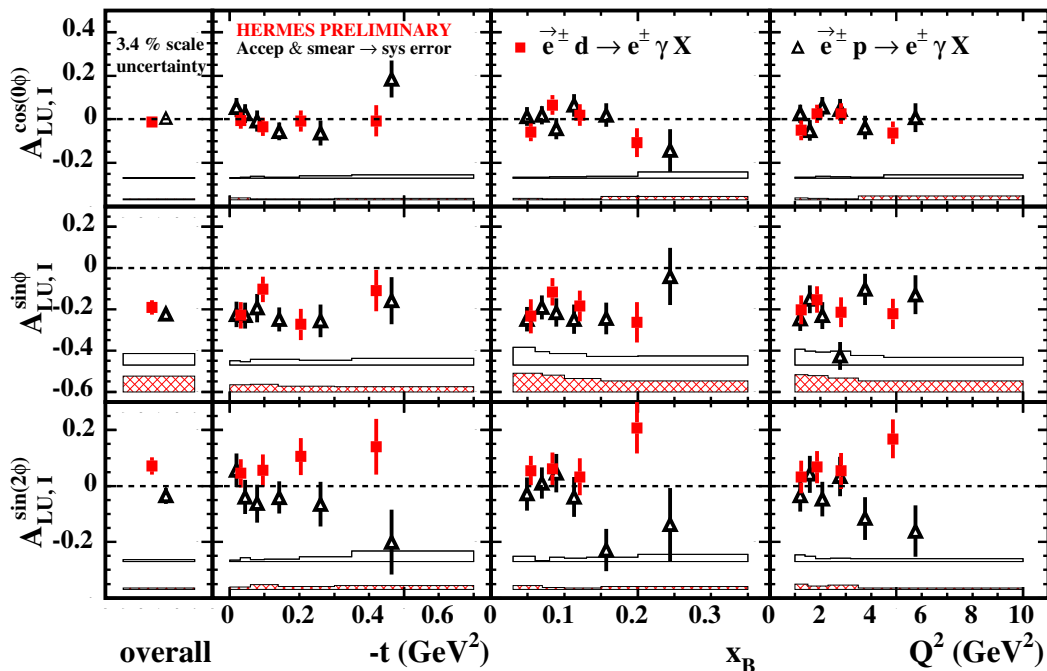
Figure 4: The amplitudes of the beam-helicity asymmetry that are sensitive to the interference term, extracted from deuteron data (squares) and from proton data (triangles) [5]. The error bars (bands) represent the statistical (systematic) uncertainties.

The nuclear-mass dependence of beam-helicity azimuthal asymmetries has been measured for targets ranging from hydrogen to xenon [7]. For hydrogen, krypton and xenon, data were taken with both beam charges. For both DVCS and BH, coherent scattering occurs at small values of $-t$ and rapidly diminishes with increasing $|t|$. Coherent and incoherent-enriched samples are selected according to a $-t$ threshold that is chosen to vary with the target such that for each sample approximately the same kinematic conditions are obtained for all target types. The nuclear-mass dependence of the beam-charge and beam-helicity azimuthal asymmetries is presented separately for the coherent and incoherent-enriched samples in Figs. 5 and 6. The $\cos\phi$ amplitude of the beam-charge asymmetry is consistent with zero for the coherent-enriched samples for all three targets, while it is about 0.1 for the incoherent-enriched samples. The $\sin\phi$ amplitude of the beam-helicity asymmetry shown in Fig. 6 has values of about -0.2 for both the coherent and incoherent-enriched samples. No nuclear-mass dependence of the beam-charge and beam-helicity asymmetries is observed within experimental uncertainties. This is in agreement with models that approximate nuclear GPDs by nucleon GPDs neglecting bound state effects. The data do not support the enhancement of nuclear asymmetries compared to the free proton asymmetries for coherent scattering on spin-0 and spin-1/2 nuclei as anticipated by various models [8, 9, 10]. They also contradict the predicted strong A dependence of the beam-charge asymmetry resulting from a contribution of meson exchange between nucleons to the scattering amplitude [10].
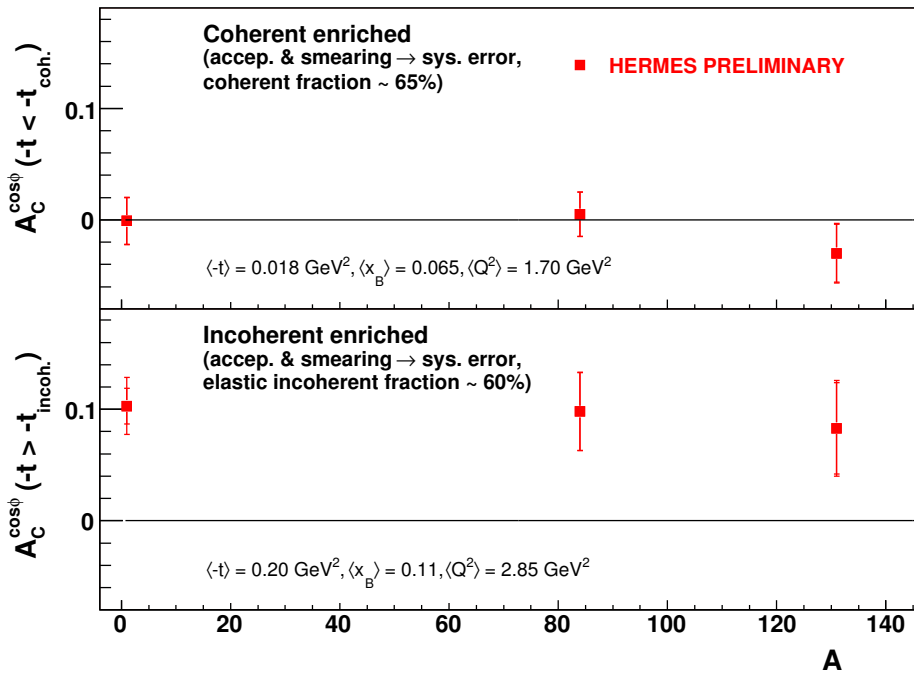
Figure 5: Nuclear-mass dependence of the $\cos\phi$ amplitude of the beam-charge asymmetry for the coherent-enriched (upper panels) and incoherent-enriched (lower panels) data samples. The inner (full) errors bar represent the statistical (total) uncertainties.

5 The HERMES Recoil Detector

In the results presented above, DVCS events were selected without detection of recoiling particles using missing-mass method. In order to ensure exclusivity and reduce the background from the associated BH process, a recoil detector was installed at HERMES in winter of 2005–2006. The recoil detector consists of a silicon strip detector, a scintillating fiber tracker and a photon detector located in a 1 T solenoidal magnetic field. The main task of the photon detector is to detect photons from π^0 decay and thereby suppress the contribution from associated Δ^+ production. The recoil detector was in operation during the high luminosity run of HERA using unpolarized hydrogen and deuterium targets from 2006 to 2007. A rich data set was collected in these two years and is being analyzed.

6 Conclusion

HERMES has made significant measurements of cosine moments of beam-charge asymmetry and sine moments of charge dependent beam-helicity asymmetry in DVCS from hydrogen and deuterium targets. The statistical precision of the data allows to put constraints on theoretical calculations. The unknown contribution from the associated process can be understood from data taken with the recoil detector. A model-dependent constraint on the total angular mo-
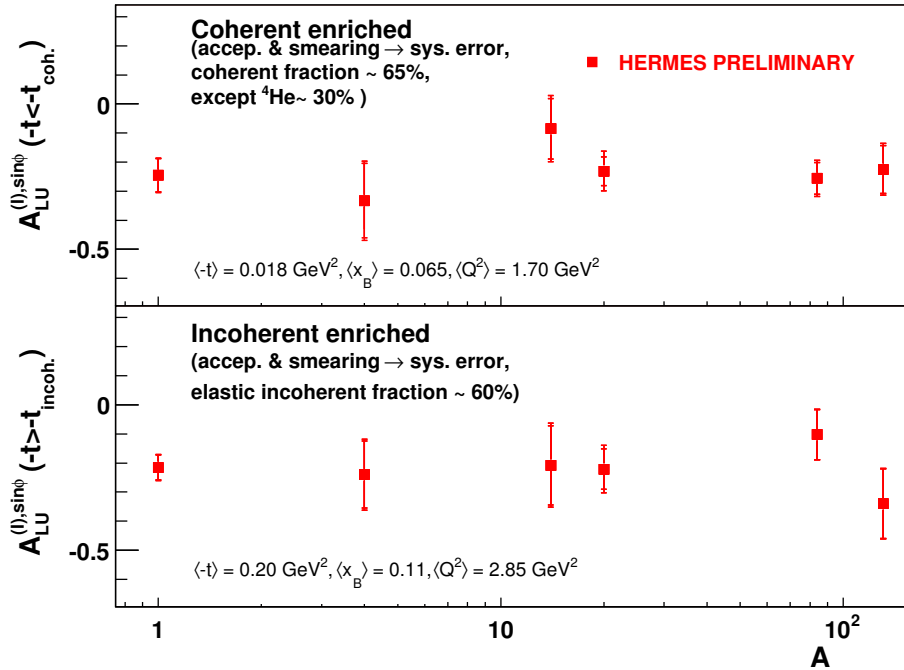
Figure 6: Nuclear-mass dependence of the $\sin\phi$ amplitude of the beam-helicity asymmetry for the coherent-enriched (upper panels) and incoherent-enriched (lower panels) data samples. The inner (full) errors bar represent the statistical (total) uncertainties.

menta carried by up and down quarks of the nucleon is obtained by comparing GPD model calculations with the measured BCA and TTSA. Beam-charge and beam-helicity asymmetries have been measured for targets ranging from hydrogen to xenon. No nuclear-mass dependence of the asymmetry amplitudes is observed within experimental uncertainties. The obtained results provide constraints on nuclear GPD models.

References

[1] A. V. Belitsky, D. Müller and A. Kirchner, Nucl. Phys. **B629** 323 (2002).

[2] A. Airapetian *et al.* [HERMES Collaboration], JHEP **06** 066 (2008).

[3] K. Ackerstaff *et al.* [HERMES Collaboration], Nucl. Instrum. Meth. **A417** 230 (1998).

[4] D. Zeiler on behalf of the HERMES Collaboration, Proc. of DIS08, London, England.

[5] H. Marukyan on behalf of the HERMES Collaboration, AIP Conf. Proc. **1149** 619 (2009).

[6] M. Vanderhaeghen, P. A. M. Guichon, and M. Guidal, Phys. Rev. **D60** 094017 (1999).

[7] H. Ye on behalf of the HERMES Collaboration, Proc. of DIS08, London, England.

[8] A. Kirchner, D. Müller, Eur. Phys. J. **C32** 347 (2003).

[9] V. Guzey, M. I. Strikman, Phys. Rev. **C68** 015204 (2003).

[10] V. Guzey, M. Siddikov, J. Phys. **G32** 251 (2006).